OL Organic Letters

pubs.acs.org/OrgLett

Letter

# Enantioselective Intramolecular Iridium-Catalyzed Cyclopropanation of α-Carbonyl Sulfoxonium Ylides

Lucas Vidal, Pan-Pan Chen, Eva Nicolas, Andrew Hackett, Craig M. Robertson, Kendall N. Houk, and Christophe Aïssa*

Cite This: *Org. Lett.* 2022, 24, 8503–8508

Read Online

ACCESS | Metrics & More | Article Recommendations | Supporting Information

**ABSTRACT:** Enantioselective cyclopropanation of α-carbonyl sulfoxonium ylides (SY) has so far been limited to addition/ring closure reactions on electron-poor olefins. Herein, we report the iridium-catalyzed intramolecular cyclopropanation of SY in the presence of a chiral diene in up to 96% yield and 98% enantioselectivity. Moreover, density functional theory calculations suggest that the *re* face of the olefin preferably attacks an iridium carbene intermediate in an asynchronous concerted step that is independent of the geometry of the olefin.

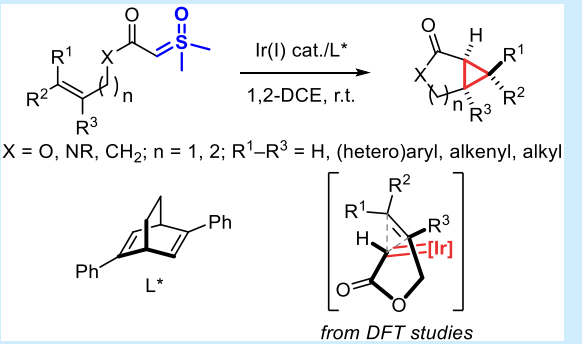




The superior safety profile of α-carbonyl sulfoxonium ylides compared to that of their diazo counterpart has recently spurred the exploration of numerous metal-catalyzed reactions in which a metal-carbene has been proposed to be a pivotal intermediate.[1] In this context, it is striking that enantioselective cyclopropanation of olefins by the intermediacy of a chiral metal-carbene, a hallmark of metal-carbene chemistry,[2] has never been observed in metal-catalyzed reactions of α-carbonyl sulfoxonium ylides. Specifically, reports of cyclopropanation of α-carbonyl sulfoxonium ylides are limited to an arene C−H activation/cyclopropanation cascade with electron-poor allenes[3] and enantioselective addition/ring closure on electron-poor olefins in the presence of either a chiral organocatalyst[4] or a chiral Lewis acid (Scheme 1a).[5] Thus, overcoming these limitations and expanding the scope of cyclopropanation of α-carbonyl sulfoxonium ylides beyond electron-poor olefins would improve our understanding of the reactivity of these ylides in homogeneous catalysis and benefit molecular science in view of the importance of cyclopropanes in drugs,[6] natural products,[7] and fragrances.[8]

Iridium(I) complexes are versatile catalysts in a diverse set of reactions of sulfoxonium ylides such as X−H (X = B, N, O, or S) insertions[9] and aromatic substitutions[10] that all likely rely on an iridium carbene intermediate. We therefore hypothesized that Ir(I) catalysts would be good candidates for promoting the cyclopropanation of α-carbonyl sulfoxonium ylides with olefins that are not activated by an electron-withdrawing group. Moreover, we reasoned that chiral diene ligands would offer an ideal platform for the development of an enantioselective version of the reaction.[11]

**Scheme 1. Enantioselective Cyclopropanation of α-Carbonyl Sulfoxonium Ylides**

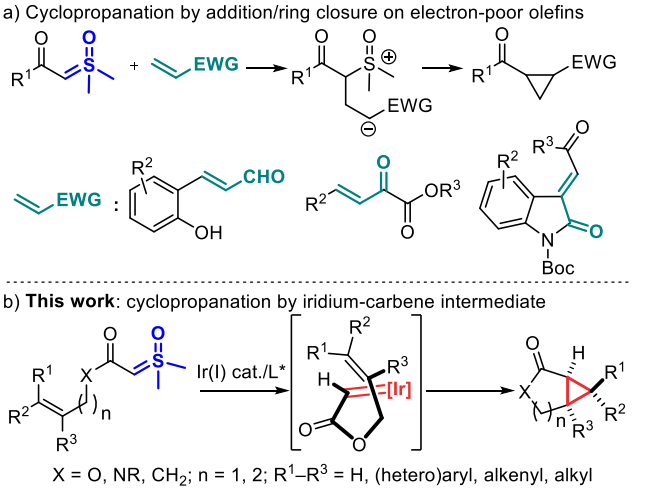


Herein, we validate this hypothesis with the asymmetric synthesis of bicyclic lactones, lactams, and ketones by intramolecular cyclopropanation of sulfoxonium ylides

**Received:** October 5, 2022
**Published:** November 11, 2022

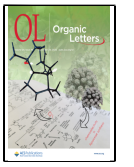





https://doi.org/10.1021/acs.orglett.2c03396
*Org. Lett.* 2022, 24, 8503−8508

(Scheme 1b). In addition, a stereochemical model supported by DFT calculations is proposed to explain how the enantioselectivity remains high regardless of the geometry of the olefin, in contrast with the known metal-catalyzed intramolecular cyclopropanations of allyl diazo acetates that have been optimized specifically for either the *E* or the *Z* olefins.[12,13]

At the beginning of our study, it became rapidly apparent during the optimization of the reaction that it was necessary to add sulfoxonium ylide **1a** slowly on a solution of the catalyst to avoid the formation of dimeric products. Under these conditions, and using $[Ir(cod)Cl]_2$ (cod = cyclooctadiene) as a catalyst in 1,2-DCE (1,2-dichloroethane) at 80 °C, we obtained bicyclic lactone (±)-**2a** in 94% yield (eq 1). Other iridium and rhodium catalysts led to lower yields, and using $Rh_2(OAc)_4$ notably led to only traces of (±)-**2a** (see Table S1).

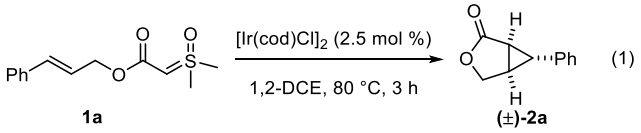

(1)

Moreover, during the initial optimization of the reaction, we noted that decreasing the temperature to 40 °C led to incomplete conversion after the slow addition of the substrate. Nevertheless, we reckoned that the catalyst was still active at this stage and that full conversion could be reached by longer exposure. We were pleased to verify this hypothesis and observed full conversion of **1a** to (−)-**2a** with 84% ee when commercially available (*R*,*R*)-**3** was used as the ligand (Table 1, entry 1). After other chiral dienes such as **4**−**8** had been examined, (*R*,*R*)-**3** remained the best ligand, and (−)-**2a** could be obtained in 90% ee when the reaction was conducted at room temperature (Table 1, entry 4 vs entries 2, 3, and 5−7).

With these optimized conditions in hands, we examined their generality on α-carbonyl sulfoxonium ylides **1a**−**o** and were delighted to obtain the envisioned racemic bicyclic lactones, lactams, and ketones in 32−98% yields (Scheme 2). Thus, (hetero)aryl substituents were well tolerated [(±)-**2a**−**d**], as were alkenyl [(±)-**2e**] and alkyl substituents [(±)-**2k**]. Moreover, *Z* olefins led to the expected cyclopropanes with an only slight decrease in yield in the case of (±)-**2f**−**h** or in identical yield in the case of trisubstituted olefins that gave (±)-**2i** and (±)-**2j**. Another trisubstituted substrate **1l** gave (±)-**2l** in 70% yield. In addition to lactones, other tethers were efficient and bicyclic ketone (±)-**2m** and lactam (±)-**2n** were obtained in 98% and 86% yields, respectively. However, six-membered ring lactone (±)-**2o** could be obtained in only 32% yield.

Then, using (*R*,*R*)-**3** as the chiral ligand and under the conditions optimized for the asymmetric variant of this cyclopropanation, we obtained the enantioenriched products in 34−96% yields and 52−98% ee (Scheme 2).[14] The best results were obtained with aryl-substituted olefins, whereas a pyrazole [(−)-**2d**], an alkenyl [(−)-**2e**], or an alkyl [(−)-**2k**] substituent was more detrimental to the enantioselectivity. Remarkably, when comparing the results of the enantioselective cyclopropanation of **1a** and its *Z* isomer **2f**, we established that the enantioselectivity remained high for both geometrical isomers of the olefin to give (−)-**2a** and (+)-**2f** with 90% ee.[15] This observation is in strong contrast with the

**Table 1. Optimization of the Enantioselectivity**[a]

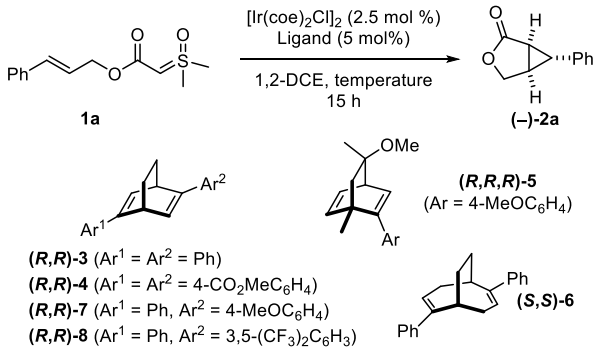


| entry | ligand | *T* (°C) | yield[c] (%) | ee[d] (%) |
|---|---|---|---|---|
| 1 | (*R*,*R*)-**3** | 40[b] | 92 | 84 |
| 2 | (*R*,*R*)-**4** | 40[b] | 80 | 78 |
| 3 | (*R*,*R*,*R*)-**5** | 40[b] | 99 | 30 |
| 4 | (*R*,*R*)-**3** | 24 | 89[e] | 90[f] |
| 5 | (*S*,*S*)-**6** | 24 | 21 | 0 |
| 6 | (*R*,*R*)-**7** | 24 | 86 | 87 |
| 7 | (*R*,*R*)-**8** | 24 | 75[e] | 75[f] |

[a]Slow addition of a solution of **1a** (0.2 mmol) in 1,2-DCE (3 mL) to the metal catalyst and ligand in 1,2-DCE (9 mL) under $N_2$ over 3 h and then stirring at the indicated temperature for 12 h. coe = cyclooctaene. [b]Temperature of the heating block. [c]Yield determined by $^1H$ NMR of the crude with 1,3,5-trimethoxybenzene as the internal standard except where otherwise indicated. [d]Enantiomeric excess of the crude material determined by HPLC. [e]Yield of the isolated product. [f]Enantiomeric excess of the isolated product determined by HPLC.

catalyzed reactions that have been developed to give optimal results with either the *E* or the *Z* isomer of allyl diazo acetates, but not with both (Table S2).[12,13] Other pairs of geometrical isomers such as **1b** and **1g**, **1c** and **1h**, and **1i** and **1j** gave equally good results when treated with the chiral Ir-diene catalyst. The enantioselectivity remained high for bicyclic ketone (−)-**2m** and for six-membered lactone (−)-**2o**, but lactam (−)-**2n** was obtained with lower enantioselectivity.

Stereochemical models were evaluated by DFT calculations[16] to understand the origins of the enantioselectivity observed in those reactions (Scheme 3). Iridium-carbenes **I** and **II** are most likely formed from **1a** and **1f**, respectively, under the reaction conditions (Scheme 3a).[9] In the reactive conformers of **I** and **II** that connect with the transition states leading to the observed products, the C−Ir bond length [1.85 Å (**I** and **II**)] and the dihedral angle between the carbon−iridium bond and the carbonyl [$\theta$ = 287° (**I**), and $\theta$ = 309° (**II**)] are similar to those measured in an isolated iridium(I)-carbene formed from the reaction of $[Ir(cod)Cl]_2$ and methyl 2-diazo-2-phenylacetate.[17] Significantly, we found that a perpendicular approach of the olefin with respect to the iridium-carbene in **TS1** and **TS3** is favored over a parallel approach in **TS2** and **TS4**. Thus, **TS1** is favored over **TS2** by 1.3 kcal $mol^{-1}$ in the case of *E* olefin **1a**, whereas **TS3** is favored over **TS4** by 6.0 kcal $mol^{-1}$ in the case of *Z* olefin **1f**. In all cases, the tether is pointing toward the less sterically congested quadrant of the $C_2$-symmetrical ligand (Scheme 3b). In addition, the C1−C2 and C1−C3 bonds of (−)-**2a** and (+)-**2f** are formed in an asynchronous concerted mechanism from **TS1** and **TS3**, respectively. In contrast, **TS2** and **TS4** are the highest-energy transition states of a two-step mechanism in


https://doi.org/10.1021/acs.orglett.2c03396
Org. Lett. 2022, 24, 8503−8508

**Scheme 2. Enantioselective Intramolecular Iridium-Catalyzed Cyclopropanation of α-Carbonyl Sulfoxonium Ylides[d]**

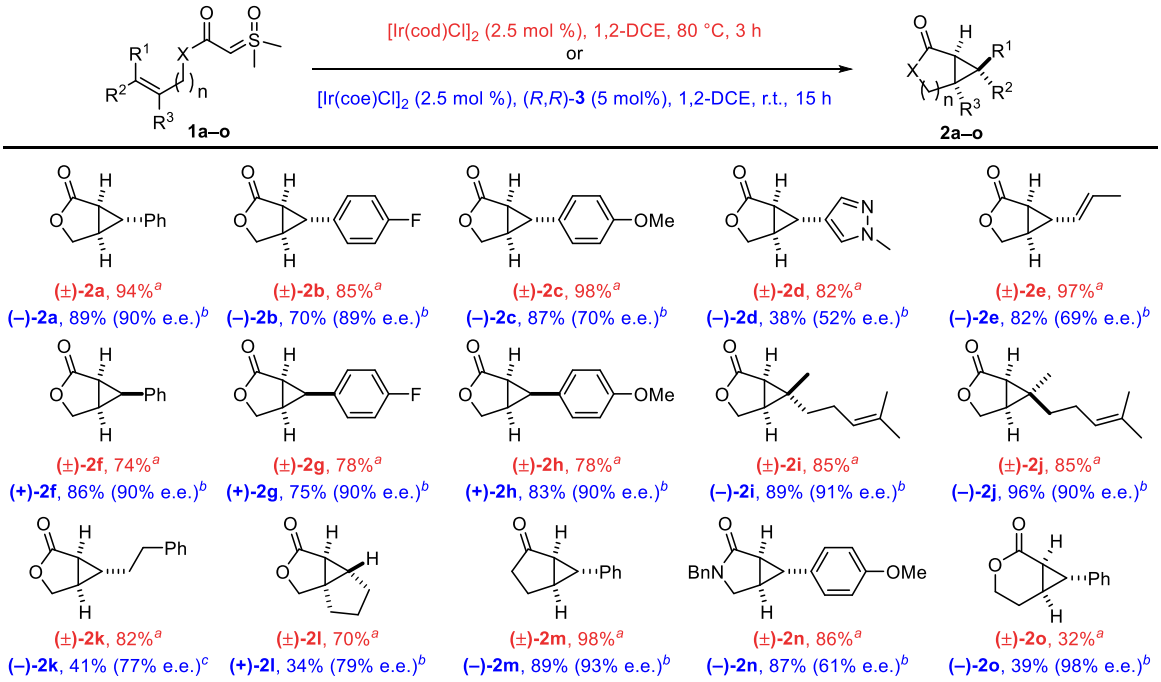


[a]Under the conditions of eq 1. [b]As in entry 4 of Table 1. [c]Slow addition for 9 h and stirring for 96 h. [d]Yields and ee's of the isolated product.

**Scheme 3. Stereochemical Model[a]**

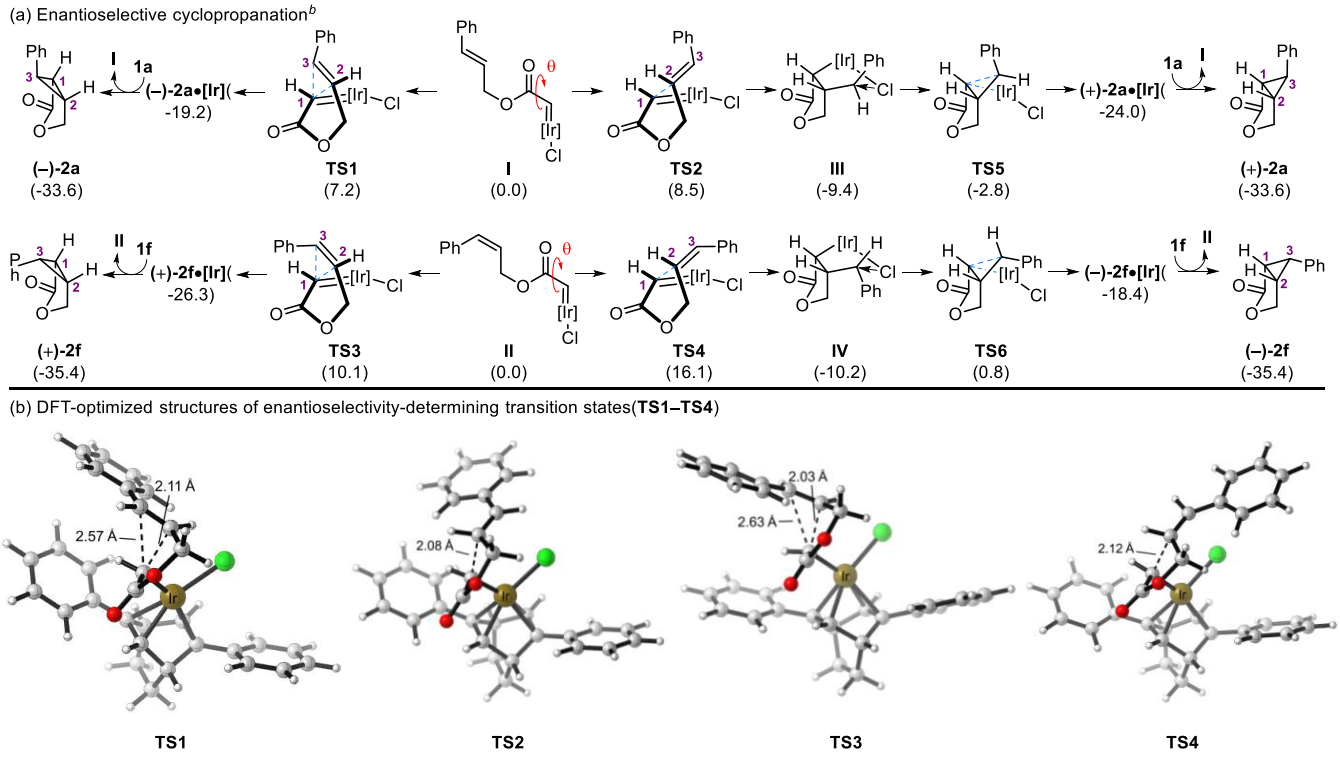


[a]Computational method: M06/def2-TZVPP-SMD(dichloromethane)//B3LYP-D3/def2-SVP. [b]Ligand omitted for the sake of clarity; energies (ΔG) are in kilocalories per mole.

which the C1−C2 bond is formed first to give intermediates **III** and **IV**, before eventually leading to the minor enantiomers through **TS5** and **TS6**. Moreover, a distortion−interaction analysis[18,19] shows that the enantioselectivity mainly arises from a greater distortion in the substrate in least favored transition states **TS2** and **TS4** (Table 2). The origins of the substrate distortion were investigated through independent gradient model analysis.[20] It revealed a stabilizing π interaction between the C1−H bond of the substrate and one of the phenyl rings of the ligand in **TS1**−**TS4**. However, maintaining



https://doi.org/10.1021/acs.orglett.2c03396
Org. Lett. 2022, 24, 8503−8508

**Table 2. Distortion–Interaction Analysis**[a]

| | $\Delta E_{dist(cat)}$ | $\Delta E_{dist(sub)}$ | $\Delta E_{int}$ | $\Delta E_{act}$ |
|---|---|---|---|---|
| **TS1** | 13.2 | −10.9 | −82.9 | −80.6 |
| **TS2** | 13.8 | 1.0 | −92.7 | −77.9 |
| $\Delta\Delta E$(**TS2**−**TS1**) | 0.6 | 11.9 | −9.8 | 2.7 |
| **TS3** | 13.0 | −12.1 | −78.9 | −78.0 |
| **TS4** | 13.2 | 3.8 | −88.6 | −71.6 |
| $\Delta\Delta E$(**TS4**−**TS3**) | 0.2 | 15.9 | −9.7 | 6.4 |

[a]Distortion–interaction analysis was performed at the M06/def2-TZVPP//B3LYP-D3/def2-SVP level of theory. Energies are in kilocalories per mole. The details of distortion–interaction analysis are provided in the Supporting Information.

that favorable C–H···$\pi$ interaction in **TS2** and **TS4** comes at the cost of greater steric hindrance,[21] and hence greater distortion, within the substrate. Overall, the DFT calculations suggest that the *re* face of the olefin is attacked preferentially in **TS1** and **TS3**, in agreement with our experimental results.

Finally, as mentioned in the introduction, cyclopropanes are important motifs in drugs, and we could demonstrate the synthetic utility of the products obtained in this study by converting (±)-**2d** into (±)-**9**, which displays the same cyclopropane substitution pattern as (±)-**10**, a nanomolar inhibitor of hematopoietic kinase 1 (Scheme 4).[22]

**Scheme 4. Potential Synthetic Utility**

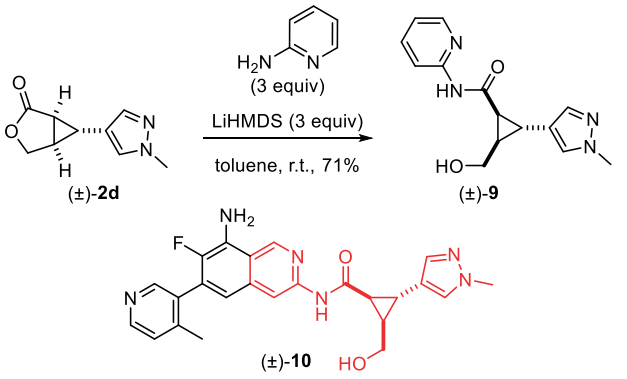


In conclusion, we have demonstrated the first example of enantioselective intramolecular cyclopropanation of $\alpha$-carbonyl sulfoxonium ylides in the presence of a chiral iridium catalyst. Hence, the method enables access to enantioenriched bicyclic lactones, lactams, and ketones. This strategy expands the scope of cyclopropanation of $\alpha$-carbonyl sulfoxonium ylides that had so far been limited to addition/ring closure reactions on electron-poor olefins. Moreover, DFT calculations revealed that an orthogonal approach of the *re* face of the olefin to an iridium carbene intermediate is preferred regardless of the geometry of the olefin, while the distortion of the substrate in the transition states is the main differentiating factor that determines the enantioselectivity.

## ■ ASSOCIATED CONTENT

### Data Availability Statement

The data underlying this study are available in the published article and its online Supporting Information.

### Supporting Information

The Supporting Information is available free of charge at https://pubs.acs.org/doi/10.1021/acs.orglett.2c03396.

Experimental procedures, crystallographic data, chiral HPLC traces, NMR spectra, and details of computational studies (PDF)

### Accession Codes

CCDC 2208521–2208522 contain the supplementary crystallographic data for this paper. These data can be obtained free of charge via www.ccdc.cam.ac.uk/data_request/cif, or by emailing data_request@ccdc.cam.ac.uk, or by contacting The Cambridge Crystallographic Data Centre, 12 Union Road, Cambridge CB2 1EZ, UK; fax: +44 1223 336033.

## ■ AUTHOR INFORMATION


### Corresponding Author

**Christophe Aïssa** − *Department of Chemistry, University of Liverpool, Liverpool L69 7ZD, United Kingdom;* orcid.org/0000-0003-0750-9435; Email: aissa@liverpool.ac.uk

### Authors

**Lucas Vidal** − *Department of Chemistry, University of Liverpool, Liverpool L69 7ZD, United Kingdom*

**Pan-Pan Chen** − *Department of Chemistry and Biochemistry, University of California, Los Angeles, California 90095, United States*

**Eva Nicolas** − *Department of Chemistry, University of Liverpool, Liverpool L69 7ZD, United Kingdom*

**Andrew Hackett** − *Department of Chemistry, University of Liverpool, Liverpool L69 7ZD, United Kingdom;* Present Address: A.H.: School of Biological Sciences, Faculty of Biology, Medicine and Health, Manchester Academic Health Science Centre, University of Manchester, Manchester M13 9PT, United Kingdom

**Craig M. Robertson** − *Department of Chemistry, University of Liverpool, Liverpool L69 7ZD, United Kingdom*

**Kendall N. Houk** − *Department of Chemistry and Biochemistry, University of California, Los Angeles, California 90095, United States;* orcid.org/0000-0002-8387-5261

Complete contact information is available at: https://pubs.acs.org/10.1021/acs.orglett.2c03396


### Author Contributions

This paper was written through contributions of L.V., P.-P.C., K.N.H., and C.A. L.V., E.N., and A.H. carried out the experimental work. P.-P.C. carried out the computational work. C.M.R. acquired and analyzed the X-ray data. K.N.H. supervised the computational work. C.A. conceived the project. All authors have given approval to the final version of the manuscript.

### Notes

The authors declare no competing financial interest.

## ■ ACKNOWLEDGMENTS

The authors are grateful to the National Science Foundation (CHE-1764328 to K.N.H.) for financial support of this research. Calculations were performed on the IDRE Hoffman2 cluster at the University of California, Los Angeles, and the Extreme Science and Engineering Discovery Environment (XSEDE), which is supported by the National Science Foundation (OCI-1053575). The authors thank the University of Liverpool for a studentship to L.V.

## REFERENCES


(1) (a) Vaitla, J.; Bayer, A. Sulfoxonium ylide derived metal carbenoids in organic synthesis. *Synthesis* **2019**, *51*, 612−628. (b) Wu, X.; Sun, S.; Yu, J. T.; Cheng, J. Recent applications of α-carbonyl sulfoxonium ylides in rhodium- and iridium-catalyzed C−H functionalizations. *Synlett* **2019**, *30*, 21−29. (c) Bisag, G. D.; Ruggieri, S.; Fochi, M.; Bernardi, L. Sulfoxonium ylides: simple compounds with chameleonic reactivity. *Org. Biomol. Chem.* **2020**, *18*, 8793−8809. (d) Kumar, A.; Sherikar, M. S.; Hanchate, V.; Prabhu, K. R. Application of sulfoxonium ylide in transition-metal-catalyzed C−H bond activation and functionalization reactions. *Tetrahedron* **2021**, *101*, 132478. (e) Caiuby, C. A. D.; Furniel, L. G.; Burtoloso, A. C. B. Asymmetric transformations from sulfoxonium ylides. *Chem. Sci.* **2022**, *13*, 1192−1209. (f) Bhorali, P.; Sultana, S.; Gogoi, S. Recent Advances in Metal-Catalyzed C−H Bond Functionalization Reactions of Sulfoxonium Ylides. *Asian J. Org. Chem.* **2022**, *11*, e202100754.

(2) (a) Lebel, H.; Marcoux, J.-F.; Molinaro, C.; Charette, A. B. Stereselective Cyclopropanation Reactions. *Chem. Rev.* **2003**, *103*, 977−1050. (b) Bartoli, G.; Bencivenni, G.; Dalpozzo, R. Asymmetric Cyclopropanation Reactions. *Synthesis* **2014**, *46*, 979−1029.

(3) Lou, J.; Wang, Q.; Zhou, Y. G.; Yu, Z. Rhodium (III)-Catalyzed Annulative Coupling of Sulfoxonium Ylides and Allenoates: An Arene C−H Activation/Cyclopropanation Cascade. *Org. Lett.* **2019**, *21*, 9217−9222.

(4) Bisag, G. D.; Pecchini, P.; Mancinelli, M.; Fochi, M.; Bernardi, L. Sulfoxonium Ylides in Aminocatalysis: An Enantioselective Entry to Cyclopropane-Fused Chromanol Structures. *Org. Lett.* **2022**, *24*, 5468−5473.

(5) (a) Wang, L.; Cao, W.; Mei, H.; Hu, L.; Feng, X. Catalytic Asymmetric Synthesis of Chiral Spiro-cyclopropyl Oxindoles from 3-Alkenyl-oxindoles and Sulfoxonium Ylides. *Adv. Synth. Catal.* **2018**, *360*, 4089−4093. (b) Pian, J.; Chen, Q.; Luo, Y.; Zhao, Z.; Liu, J.; He, L.; Li, S.-W. Asymmetric Synthesis of Chiral Cyclopropanes from Sulfoxonium Ylides Catalyzed by a Chiral-at-Metal Rh(III) Complex. *Org. Lett.* **2022**, *24*, 5641−5645.

(6) Talele, T. T. The "Cyclopropyl Fragment" is a Versatile Player that Frequently Appears in Preclinical/Clinical Drug Molecules. *J. Med. Chem.* **2016**, *59*, 8712−8756.

(7) Fan, Y.-Y.; Gao, X.-H.; Yue, J.-M. Attractive natural products with strained cyclopropane and/or cyclobutane ring systems. *Science China Chemistry* **2016**, *59*, 1126−1141.

(8) Schröder, F. Present and Future of Cyclopropanations in Fragrance Chemistry. *Chemistry & Biodiversity* **2014**, *11*, 1734−1751.

(9) (a) Mangion, I. K.; Nwamba, I. K.; Shevlin, M.; Huffman, M. A. Iridium-catalyzed X− H insertions of sulfoxonium ylides. *Org. Lett.* **2009**, *11*, 3566−3569. (b) Vaitla, J.; Bayer, A.; Hopmann, K. H. Synthesis of indoles and pyrroles utilizing iridium carbenes generated from sulfoxonium ylides. *Angew. Chem., Int. Ed.* **2017**, *56*, 4277−4281. (c) Phelps, A. M.; Chan, V. S.; Napolitano, J. G.; Krabbe, S. W.; Schomaker, J. M.; Shekhar, S. Ligand-controlled synthesis of azoles via Ir-catalyzed reactions of sulfoxonium ylides with 2-amino heterocycles. *J. Org. Chem.* **2016**, *81*, 4158−4169. (d) Li, J.; He, H.; Huang, M.; Chen, Y.; Luo, Y.; Yan, K.; Wang, Q.; Wu, Y. Iridium-Catalyzed B−H Bond Insertion Reactions Using Sulfoxonium Ylides as Carbene Precursors toward α-Boryl Carbonyls. *Org. Lett.* **2019**, *21*, 9005−9008. (e) Zhang, S.-S.; Xie, H.; Shu, B.; Che, T.; Wang, X.-T.; Peng, D.; Yang, F.; Zhang, L. Iridium-catalyzed B−H insertion of sulfoxonium ylides and borane adducts: a versatile platform to α-boryl carbonyls. *Chem. Commun.* **2020**, *56*, 423−426.

(10) (a) Clare, D.; Dobson, B. C.; Inglesby, P. A.; Aïssa, C. Chemospecific Cyclizations of α-Carbonyl Sulfoxonium Ylides on Aryls and Heteroaryls. *Angew. Chem., Int. Ed.* **2019**, *58*, 16198−16202. (b) Caiuby, C. A. D.; de Jesus, M. P.; Burtoloso, A. C. B. α-Imido Iridium Carbenes from Imidoyl Sulfoxonium Ylides: Application in the One-Step Synthesis of Indoles. *J. Org. Chem.* **2020**, *85*, 7433−7445.

(11) Hirano, M.; Komine, N.; Arata, E.; Gridneva, T.; Hatori, A.; Kaizawa, N.; Kamakura, K.; Kuramochi, A.; Kurita, S.; Machida, S.; Okada, H.; Sawa-saki, A.; Uchino, T. Recent advances of achiral and chiral diene ligands in transition-metal catalysis. *Tetrahedron Lett.* **2019**, *60*, 150924.

(12) For examples with *E* olefins: (a) Uchida, T.; Katsuki, T. α-Diazoacetates as Carbene Precursors: Metallosalen-Catalyzed Asymmetric Cyclopropanation. *Synthesis* **2006**, *2006*, 1715−1723. (b) Langlotz, B. K.; Wadepohl, H.; Gade, L. H. Chiral bis-(pyridylimino)isoindoles: a highly modular class of pincer ligands for enantioselective catalysis. *Angew. Chem., Int. Ed.* **2008**, *47*, 4670−4674. (c) Xu, Z. J.; Fang, R.; Zhao, C.; Huang, J. S.; Li, G. Y.; Zhu, N.; Che, C. M. *cis*-β-Bis(carbonyl) ruthenium−salen complexes: X-ray crystal structures and remarkable catalytic properties toward asymmetric intramolecular alkene cyclopropanation. *J. Am. Chem. Soc.* **2009**, *131*, 4405−4417. (d) Abu-Elfotoh, A. M.; Phomkeona, K.; Shibatomi, K.; Iwasa, S. Asymmetric Inter-and Intramolecular Cyclopropanation Reactions Catalyzed by a Reusable Macroporous-Polymer-Supported Chiral Ruthenium (II)/Phenyloxazoline Complex. *Angew. Chem., Int. Ed.* **2010**, *49*, 8439−8443. (e) Xu, X.; Lu, H.; Ruppel, J. V.; Cui, X.; Lopez de Mesa, S.; Wojtas, L.; Zhang, X. P. Highly asymmetric intramolecular cyclopropanation of acceptor-substituted diazoacetates by Co (II)-based metalloradical catalysis: iterative approach for development of new-generation catalysts. *J. Am. Chem. Soc.* **2011**, *133*, 15292−15295.

(13) For examples with *Z* olefins: (a) Doyle, M. P.; Austin, R. E.; Bailey, A. S.; Dwyer, M. P.; Dyatkin, A. B.; Kalinin, A. V.; Kwan, M. M.; Liras, S.; Oalmann, C. J. Enantioselective intramolecular cyclopropanations of allylic and homoallylic diazoacetates and diazoacetamides using chiral dirhodium (II) carboxamide catalysts. *J. Am. Chem. Soc.* **1995**, *117*, 5763. (b) Li, G. Y.; Zhang, J.; Chan, P. W. H.; Xu, Z. J.; Zhu, N.; Che, C. M. Enantioselective intramolecular cyclopropanation of cis-alkenes by chiral ruthenium (II) Schiff base catalysts and crystal structures of (Schiff base) ruthenium complexes containing carbene, $PPh_3$, and CO ligands. *Organometallics* **2006**, *25*, 1676−1688.

(14) The reaction was also conducted on a 1 mmol scale of **1a** using $[((R,R)\text{-}\mathbf{3})IrCl]_2$ as a catalyst to give (−)-**2a** in 91% yield and 93% ee.

(15) The absolute configuration of (−)-**2a** and (+)-**2f** was determined by X-ray crystallography of their *p*-bromophenyl derivatives (CCDC 2208521 and 2208522, respectively) (see the Supporting Information).

(16) Computational details are included in the Supporting Information.

(17) Tindall, D. J.; Werlé, C.; Goddard, R.; Philipps, P.; Farès, C.; Fürstner, A. Structure and reactivity of half-sandwich Rh (+3) and Ir (+3) carbene complexes. Catalytic metathesis of azobenzene derivatives. *J. Am. Chem. Soc.* **2018**, *140*, 1884−1893.

(18) For early studies related to distortion−interaction analysis, see: (a) Kitaura, K.; Morokuma, K. A New Energy Decomposition Scheme for Molecular Interactions within the Hartree-Fock Approximation. *Int. J. Quantum Chem.* **1976**, *10*, 325−340. (b) Ziegler, T.; Rauk, A. A Theoretical Study of the Ethylene-Metal Bond in Complexes between Copper(1+), Silver(1+), Gold(1+), Platinum(0) or Platinum(2+) and Ethylene, Based on the Hartree-Fock-Slater Transition-State Method. *Inorg. Chem.* **1979**, *18*, 1558−1565.

(19) For reviews of distortion−interaction analysis, see: (a) van Leeuwen, P. W. N. M.; Kamer, P. C. J.; Reek, J. N. H.; Dierkes, P. Ligand Bite Angle Effects in Metal-catalyzed C−C Bond Formation. *Chem. Rev.* **2000**, *100*, 2741−2770. (b) van Zeist, W.-J.; Bickelhaupt, F. M. The Activation Strain Model of Chemical Reactivity. *Org. Biomol. Chem.* **2010**, *8*, 3118−3127. (c) Fernández, I.; Bickelhaupt, F. M. The Activation Strain Model and Molecular Orbital Theory: Understanding and Designing Chemical Reactions. *Chem. Soc. Rev.* **2014**, *43*, 4953−4967. (d) Bickelhaupt, F. M.; Houk, K. N. Analyzing Reaction Rates with the Distortion/Interaction-Activation Strain Model. *Angew. Chem., Int. Ed.* **2017**, *56*, 10070−10086.

(20) Lefebvre, C.; Rubez, G.; Khartabil, H.; Boisson, J.-C.; Contreras-García, J.; Hénon, E. Accurately Extracting the Signature of Intermolecular Interactions Present in the NCI Plot of the Reduced Density Gradient versus Electron Density. *Phys. Chem. Chem. Phys.* **2017**, *19*, 17928−17936.




https://doi.org/10.1021/acs.orglett.2c03396
*Org. Lett.* 2022, 24, 8503−8508

(21) The greater steric hindrance in **TS2** and **TS4** is rooted in the dihedral angles between C1−H and C2−H [i.e. −106° (**TS1**), 33° (**TS2**), −98° (**TS3**), and 34° (**TS4**)], which brings the two hydrogen atoms within 2.25 Å in **TS2** and **TS4**.
(22) Chan, B.; Drobnick, J.; Gazzard, L.; Heffron, T.; Liang, J.; Malhotra, S.; Mendonca, R.; Rajapaksa, N.; Stivala, C.; Tellis, J.; Wang, W.; Wei, B.; Zhou, A.; Cartwright, M. W.; Lainchbury, M.; Gancia, E.; Seward, E.; Madin, A.; Favor, S.; Fong, C. K.; Hu, Y.; Good, A. Isoquinolines as inhibitors of hpk1. Patent WO2018183964A1, 2018.





https://doi.org/10.1021/acs.orglett.2c03396
*Org. Lett.* 2022, 24, 8503−8508